Insights into the cellular mechanism of the yeast ubiquitin ligase APC/C-Cdh1 from the analysis of in vivo degrons

Lea Arnold*, Sebastian Höckner*, and Wolfgang Seufert
Department of Genetics, University of Regensburg, D-93040 Regensburg, Germany

ABSTRACT **The anaphase-promoting complex/cyclosome (APC/C) controls a variety of cellular processes through its ability to target numerous protein substrates for timely degradation. Substrate selection by this ubiquitin ligase depends on related activator proteins, Cdc20 and Cdh1, which bind and activate the APC/C at distinct cell cycle stages. Biochemical and structural studies revealed that Cdc20 and Cdh1 carry conserved receptor domains to recognize specific sequence motifs in substrates, such as D and KEN boxes. The mechanisms for ordered degradation of APC/C substrates, however, remain incompletely understood. Here we describe minimal degradation sequences (degrons) sufficient for rapid APC/C-Cdh1–specific in vivo degradation. The polo kinase Cdc5–derived degron contained an essential KEN motif, whereas a single RxxL-type D box was the relevant signal in the Cdc20-derived degradation domain, indicating that either motif may support specific recognition by Cdh1. In both degrons, the APC/C recognition motif was flanked by a nuclear localization sequence. Forced localization of the degron constructs revealed that proteolysis mediated by APC/C-Cdh1 is restricted to the nucleus and maximally active in the nucleoplasm. Levels of Iqg1, a cytoplasmic Cdh1 substrate, decreased detectably later than the nucleus-localized Cdh1 substrate Ase1, indicating that confinement to the nucleus may allow for temporal control of APC/C-Cdh1–mediated proteolysis.**

Monitoring Editor
Orna Cohen-Fix
National Institutes of Health

Received: Sep 2, 2014
Revised: Dec 18, 2014
Accepted: Dec 19, 2014

INTRODUCTION

The anaphase-promoting complex/cyclosome (APC/C) is a conserved multisubunit E3 ubiquitin ligase that targets a multitude of protein substrates, including critical mitotic regulators for degradation by the proteasome (Barford, 2011; Primorac and Musacchio, 2013). Substrate ubiquitination by the APC/C depends on structurally related activator proteins of the Cdc20/Fizzy family, which are characterized by a conserved WD40 domain. The activator proteins contribute to substrate recognition and binding and interact with the APC/C at distinct stages of the cell cycle. The APC/C is activated by Cdc20 in metaphase to facilitate sister-chromatid separation by destruction of securin (Cohen-Fix *et al.*, 1996; Waizenegger *et al.*, 2000). APC/C-Cdc20 also initiates degradation of cyclins, thereby lowering the activity of the cyclin-dependent kinases (Cdks; Clute and Pines, 1999; Shirayama *et al.*, 1999; Wäsch and Cross, 2002). The other activator, Cdh1, binds the APC/C in late mitosis to promote mitotic exit and maintain APC/C activity during the subsequent G1 phase (Huang *et al.*, 2001). Cdh1 recognizes a broader set of substrates than Cdc20, including, among others, spindle-associated proteins, mitotic cyclins, mitotic kinases like Plk1/Cdc5, and the early activator Cdc20 (Peters, 2006).

Substrate recognition by the APC/C-activator complex is based on specific recognition signals that are present in most APC/C substrates in one or more copies. The best-defined representatives

This article was published online ahead of print in MBoC in Press (http://www.molbiolcell.org/cgi/doi/10.1091/mbc.E14-09-1342) on December 24, 2014.

*These authors contributed equally to this work.

Address correspondence to: Wolfgang Seufert (Wolfgang.Seufert@ur.de).

Abbreviations used: APC/C, anaphase-promoting complex/cyclosome; Cdk, cyclin-dependent kinase; DIC, differential interference contrast; GFP, green fluorescent protein; NES, nuclear export signal; NLS, nuclear localization sequence; SPB, spindle pole body.

are the destruction box (D box), with a consensus of RxxLxxxxN (Glotzer *et al.*, 1991), and the KEN box, named after its consensus sequence, KENxxxN (Pfleger and Kirschner, 2000). Although the KEN box is supposed to be preferred by Cdh1 (Burton and Solomon, 2001; Pfleger *et al.*, 2001), D and KEN boxes are frequently found in substrates of both Cdc20 and Cdh1. Moreover, the recently identified receptor sites for D and KEN boxes within the WD40 domain are highly conserved between Cdc20 and Cdh1 paralogues (Chao, Kulkarni, *et al.*, 2012; Tian, Li, *et al.*, 2012; He *et al.*, 2013), indicating that binding of these motifs is an elementary step in substrate recognition by the activators. Despite this notion, Cdc20 and Cdh1 seem to activate the APC/C in a substrate-specific manner (Visintin *et al.*, 1997; Schwab *et al.*, 2001). This substrate specificity is assumed to result from additional interactions between substrate and activator involving moderately conserved binding sites on the WD40 domain, as reported for binding of the pseudosubstrate inhibitor Acm1 to Cdh1 in budding yeast (He *et al.*, 2013). However, it remains unknown whether substrates also employ activator-specific interaction motifs in addition to D and KEN boxes for selective binding to either Cdc20 or Cdh1. The positions of the binding sites on the WD40 propeller suggested cooperative binding of D and KEN boxes, provided that both motifs are arranged in a certain order and distance (Chao, Kulkarni, *et al.*, 2012). Nevertheless, the distance and orientation of these motifs vary between substrates, and cooperativity between D and KEN boxes has not always been observed in vitro (Chao, Kulkarni, *et al.*, 2012; Tian, Li, *et al.*, 2012). Moreover, it is unclear whether cooperative degron binding is responsible for timing and efficiency of substrate degradation in vivo.

APC/C activity is under tight control to ensure that APC/C substrates are targeted for degradation just at the right time in the cell cycle. APC/C activation is regulated by multiple mechanisms, including Cdc20 proteolysis (Pfleger and Kirschner, 2000; Robbins and Cross, 2010), pseudosubstrate inhibition (Grosskortenhaus and Sprenger, 2002; Miller *et al.*, 2006; Burton *et al.*, 2011), and Cdk-dependent phosphorylation. Phosphorylation of APC/C subunits during mitosis stimulates binding of Cdc20 (Kramer *et al.*, 2000; Rudner and Murray, 2000). In contrast, Cdk-dependent phosphorylation of Cdh1 prevents its interaction with the APC/C (Zachariae, Schwab, *et al.*, 1998; Kramer *et al.*, 2000), thereby limiting APC/C-Cdh1 activity to late mitosis and G1 when Cdk activity is low.

In addition to regulating Cdh1 binding to the APC/C, Cdk-dependent phosphorylation was reported to cause nuclear export of Cdh1 in *Saccharomyces cerevisiae* (Jaquenoud *et al.*, 2002). Because APC/C subunits and the early activator Cdc20 were detected in the nucleus (Zachariae, Shin, *et al.*, 1996; Shirayama *et al.*, 1998; Jaquenoud *et al.*, 2002; Melloy and Holloway, 2004), it is assumed that APC/C-mediated ubiquitination occurs within the nuclear compartment and that nuclear export of Cdh1 helps inactivate the APC/C at the G1/S transition. Indeed, it was reported that degradation of the Cdc20 substrates Kip1 and Pds1 requires a nuclear localization sequence (NLS) or proteins involved in nuclear import (Bäumer *et al.*, 2000; Gordon and Roof, 2001). Similarly, an NLS was described to be required for degradation of the kinesin and Cdh1 substrate Cin8 (Hildebrandt and Hoyt, 2001), and nuclear localization of Cdh1 seems to be important for full activity of APC/C-Cdh1 (Jaquenoud *et al.*, 2002). However, several Cdh1 substrates reside both inside and outside the nucleus, such as the polo kinase Cdc5 (Charles *et al.*, 1998; Lee *et al.*, 2005) and the mitotic cyclin Clb2 (Schwab *et al.*, 1997; Hood *et al.*, 2001), or are even found exclusively outside the nucleus, such as the bud-neck proteins Iqg1 (Epp and Chant, 1997; Ko *et al.*, 2007) and Hsl1 (Barral *et al.*, 1999; Burton and Solomon, 2000). So far, it has not rigorously been tested whether cytoplasmic substrates require nuclear import for their Cdh1-dependent degradation or whether APC/C-Cdh1, even though concentrated in the nucleus, may be active in the cytoplasm as well.

In this study, we identified small N-terminal regions of both Cdc20 and Cdc5 as transferable degradation domains (degrons) that mediated efficient targeting by APC/C-Cdh1. We fused the degrons to green fluorescent protein (GFP) to study APC/C-Cdh1–dependent degradation in vivo. Our results revealed that APC/C-Cdh1–dependent degradation is maximal when substrates reside in the nucleoplasm and argue against APC/C-Cdh1 activity outside the nucleus. Moreover, we provide indications for a spatiotemporal mechanism that, in addition to the temporal control of Cdh1 binding to the APC/C, may regulate APC/C-Cdh1–dependent degradation based on the subcellular localization of substrates.

RESULTS

Short N-terminal regions of Cdc5 and Cdc20 act as APC/C-Cdh1–specific degrons

Proteins targeted for degradation by the APC/C-Cdh1 ubiquitin ligase in budding yeast include the polo kinase Cdc5 and the APC/C activator Cdc20. In both cases, N-terminal degradation signals were found to be required for instability in G1 (Charles *et al.*, 1998; Prinz *et al.*, 1998; Shirayama *et al.*, 1998; Robbins and Cross, 2010). To learn more about the degradation sequences of these proteins, we asked whether their N-terminal regions might also be sufficient for cell cycle–regulated proteolysis. To this end, amino acids 1–80 of either Cdc5 or Cdc20 (Figure 1, A and B) were fused to GFP, and the constructs were expressed from a constitutive promoter (*pTEF2*). Cells were synchronized by release from a pheromone-induced arrest in G1, and protein levels were then followed by Western analysis. Cell synchrony was assessed by analyzing the DNA content of the cell population, bud formation, and nuclear division (Figure 1, C and D). Unlike the levels of nonfused GFP, which remained constant, protein abundance of Cdc5(1-80)-GFP and Cdc20(1-80)-GFP fluctuated during the cell cycle (Figure 1, E–G). Protein levels of both constructs were minimal in G1, increased when cells entered the division cycle, reached a maximum during anaphase, and subsequently declined again to a minimum in G1. The observed fluctuation pattern resembled that of the mitotic cyclin Clb2 (Figure 1, E–G, middle), a known substrate of the APC/C (Schwab *et al.*, 2001; Wäsch and Cross, 2002). These data indicated that Cdc5(1-80) and Cdc20(1-80) are degrons sufficient for cell cycle–regulated instability.

To characterize further the observed instability, we used time-lapse fluorescence microscopy to follow the behavior of Cdc5(1-80)-GFP and Cdc20(1-80)-GFP in living cells. To this end, confocal fluorescence images of strains coexpressing the GFP fusion constructs and a nuclear Cherry marker were taken at 5-min intervals for 2 h at 22°C. Unlike nonfused GFP, which spread over the cytoplasm (Supplemental Figure S1), both Cdc5(1-80)-GFP and Cdc20(1-80)-GFP located exclusively to the nucleus (Figure 2), indicating that both degrons carry a previously unrecognized NLS.

Consistent with Western analysis, fluorescence intensities of Cdc5(1-80)-GFP and Cdc20(1-80)-GFP fluctuated during the cell cycle of wild-type cells (Figure 2, A and C). GFP signals of both fusion proteins accumulated in the nuclei of budded cells, and their fluorescence intensities remained high during nuclear division until late mitosis, from when on the GFP signals in both mother and daughter cells decreased to a minimum in the following G1 phase (Supplemental Movies 2A and 2C). Signal intensities rose again

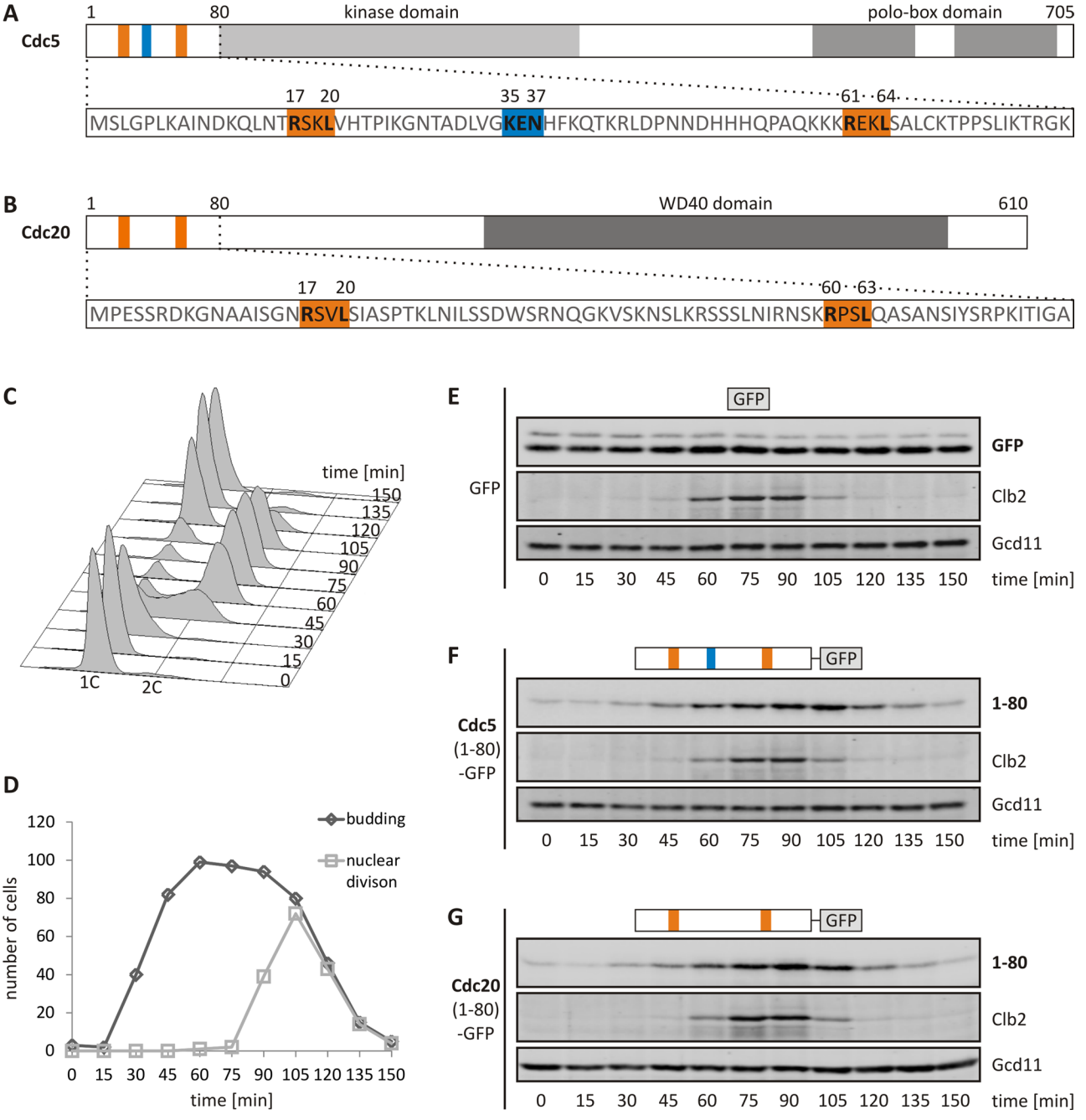

FIGURE 1: The N-terminal regions of Cdc5 and Cdc20 are degrons sufficient for cell cycle–controlled protein degradation. (A, B) Schematic domain structure of (A) the yeast polo kinase Cdc5 and (B) the yeast APC/C activator Cdc20. The amino acid sequences of the analyzed amino-terminal regions (1–80) are given below, with RxxL (orange) and KEN (blue) motifs highlighted in color. Numbers indicate amino acid positions. (C–G) Cells were synchronized for cell cycle progression by release from a pheromone-induced arrest in G1. Samples were taken at the indicated times after release from the G1 arrest. (C) The DNA content of the cell population was measured by flow cytometry. In the DNA histograms, relative fluorescence intensities are shown on the horizontal axis and cell numbers on the vertical axis. 1C, G1 cells; 2C, G2 and M cells. (D) Budding and nuclear division were determined by microscopy of DAPI-stained cells ($n = 100$). (E–G) Immunoblots showing protein levels of (E) GFP, (F) Cdc5(1-80)-GFP), and (G) Cdc20(1-80)-GFP expressed from the constitutive *TEF2* promoter. For comparison, protein levels of the endogenously expressed mitotic cyclin Clb2 were analyzed. Endogenous levels of Gcd11 served as a loading control. (E, F) GFP and Cdc5(1-80)-GFP were detected by the Myc-specific antibody 9E10 and (G) Cdc20(1-80)-GFP by a GFP-specific antibody (anti-GFP). (E–G) Gcd11 and Clb2 were detected by polyclonal rabbit antisera. DNA histogram (C), bud formation, and nuclear division (D) are representatively shown of the strain expressing Cdc5(1-80)-GFP.

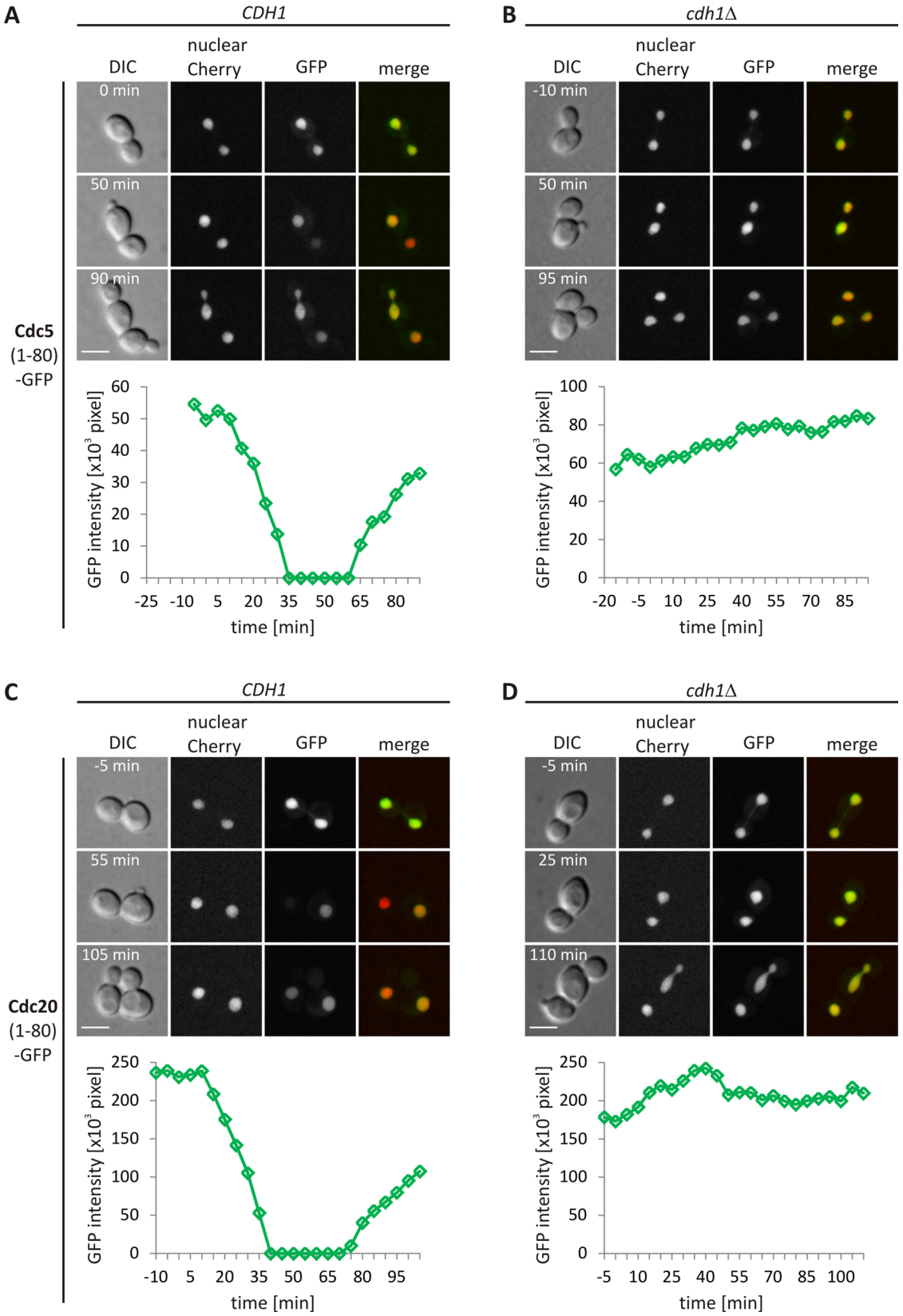

FIGURE 2: The Cdc5 and Cdc20 degron constructs reside in the nucleus and are specifically targeted by APC/C-Cdh1. (A–D) Live-cell imaging of (A, C) wild-type (*CDH1*) and (B, D) *cdh1*-deletion cells expressing (A, B) Cdc5(1-80)-GFP or (C, D) Cdc20(1-80)-GFP from the constitutive *TEF2* promoter. To visualize the nucleus, strains coexpressed a stable nuclear Cherry fusion protein. A representative cell is shown for each strain, and GFP intensity of the daughter cell was quantified for every time point indicated. Spindle breakdown, set to $t = 0$ min, was defined as the maximum distance between the separated nuclei. The horizontal axis of the diagrams shows the time, and the vertical axis represents the GFP intensity. Merge, merged Cherry and GFP images. Scale bar, 5 μm.

when cells entered a new round of cell division, which was discernible by the emergence of a new bud. We quantified the fluorescence signals in single daughter cells (diagrams in Figure 2, A and C) to estimate the in vivo degradation rates of the fusion constructs. We chose daughter cells for quantification because their longer G1 phase led to a more complete clearance of the constitutively expressed fusion proteins. Levels of both Cdc5(1-80)-GFP and Cdc20(1-80)-GFP started to decline in late mitosis at around the time of spindle breakdown, which was used to normalize the time axis. Quantification of the GFP signal revealed that degradation rates increased gradually and reached maximal values of ~10-min half-life at 22°C (Cdc5(1-80)-GFP: 10.3 ± 2.9 min; $n = 10$; Cdc20(1-80)-GFP: 10.2 ± 4.0 min; $n = 10$) in spite of constitutive expression from the *TEF2* promoter. This underlines the potency of the degradation system responsible for proteolysis of these degrons.

The period of instability of Cdc5(1-80)-GFP and Cdc20(1-80)-GFP, ranging from late mitosis to the end of G1 phase, suggested that both fusion proteins are targeted by APC/C-Cdh1. To test this hypothesis, we analyzed their abundance in strains lacking *CDH1*. In contrast to the situation in wild-type cells, fluorescence intensities of Cdc5(1-80)-GFP and Cdc20(1-80)-GFP remained high during anaphase and the subsequent G1 phase in *cdh1*Δ cells (Figure 2, B and D; Supplemental Movies 2B and 2D). Moreover, signal intensities measured in wild-type and *cdh1*Δ cells did not decline in the period before nuclear division (Supplemental Figure S2), arguing against the possibility that the fusion proteins are recognized by the early activator Cdc20. Together the timing of Cdc5(1-80)-GFP and Cdc20(1-80)-GFP degradation and their stability in *cdh1*Δ mutants indicated that both degrons are specifically targeted for destruction by Cdh1 but not by Cdc20.

A KEN box is essential for the Cdc5 degron

To define the sequence elements that are responsible for Cdh1-mediated degradation of Cdc5(1-80)-GFP, we constructed several mutant and truncated derivatives. The constructs were placed under control of a regulable promoter (*pGAL1*) to control their transcription. For these derivatives and all further fusion constructs analyzed in this study, we ensured that comparable protein levels were expressed in nonsynchronized cells to facilitate stability measurements (Supplemental Figure S3).

To analyze protein stability in G1, we expressed the fusion constructs for 2 h in pheromone-arrested cells, whose complete arrest in G1 was verified by measuring the DNA content of the cell population using flow cytometry (Supplemental Figure S4). After promoter repression, we followed protein levels by Western analysis. In addition, we visualized the constructs in nonsynchronized cells by fluorescence microscopy.

As a control, we examined nonfused GFP, which, as expected, was stable in G1-arrested cells (Figure 3A) and produced fluorescence signals of similar intensities in G1 and mitotic cells. In contrast, levels of Cdc5(1-80)-GFP dropped rapidly after promoter repression and were no longer detectable after 30 min, indicating a high degree of instability in G1 (Figure 3B). Consistently, Cdc5(1-80)-GFP showed an intense GFP signal in the nucleus of mitotic cells but was hardly detectable in unbudded G1 cells (Figure 3B).

Amino acids 1–80 of Cdc5 exhibit two RxxL motifs (RxxL1, starting at position 17; and RxxL2, starting at position 60; Figure 1A), which have been implicated in degradation of the polo-like kinase (Charles *et al.*, 1998). However, this domain also carries a KEN motif (starting at position 35; Figure 1A; Michael *et al.*, 2008), whose role in degradation has so far not been investigated. To determine the individual contributions of these elements to the function of the Cdc5 degron, we mutated the RxxL motifs and the KEN motif separately by alanine substitution mutagenesis (rxxl1/2: both RxxL to AxxA; ken: KEN to AAN). We found that mutating the KEN sequence alone led to a massive stabilization of Cdc5(1-80)-GFP in the shut-off experiment, in agreement with the accumulation of the mutant protein to high levels in the nuclei of G1 cells (Figure 3C). From these observations, we conclude that the KEN motif is an essential part of the Cdc5 degron and thus constitutes a functional KEN box.

To further define its significance for Cdc5 degradation, we mutated the KEN box within the full-length Cdc5 protein (Supplemental Figure S5). In contrast to wild-type Cdc5, the KEN box mutant version of Cdc5 accumulated to substantial levels in G1-arrested cells and slowly disappeared after promoter shut-off. When expressed in nonsynchronized cells, both the wild-type and mutant proteins accumulated to similar levels. Thus the KEN box is a major signal for the cell cycle–regulated instability of yeast Cdc5.

Consistent with a previous report (Charles *et al.*, 1998), the RxxL motifs of the Cdc5 degron also contributed to instability (Figure 3D). The simultaneous mutation of both RxxL motifs within the Cdc5(1-80)-GFP construct reduced the degradation of this fusion protein, but the stabilization was less pronounced compared with the ken mutation (Figure 3, C and D). At the same time, the rxxl1/2 mutation reduced the nuclear localization of the construct. Unlike Cdc5(1-80)-GFP, a sizable portion of the rxxl1/2 mutant version was seen in the cytoplasm (Figure 3D). This observation raised the question of whether stabilization and cytoplasmic localization of the rxxl1/2 mutant might be linked. To address this possibility, we attached a heterologous NLS derived from the transcription factor Swi5 (Moll *et al.*, 1991) to the C-terminus of the fusion protein, creating a Cdc5(1-80) rxxl1/2-GFP+NLS construct (Figure 3E). Indeed, attachment of the NLS not only restored nuclear localization, but it also reversed the stabilization caused by the rxxl1/2 mutation (Figure 3E). As a control, we also attached the NLS to otherwise nonfused GFP and found that this construct was stable in G1 (Figure 3F), arguing against the possibility that the NLS might carry an unrecognized degradation signal. Together these results suggested that localization to the cytoplasm may interfere with KEN box–mediated proteolysis of Cdc5(1-80). Thus one or both RxxL motifs appear to contribute to instability only indirectly by supporting nuclear localization of the construct. However, attachment of the NLS did not fully compensate for the rxxl1/2 mutation, since the Cdc5(1-80)rxxl1/2-GFP+NLS construct was less efficiently degraded than wild-type Cdc5(1-80)-GFP (Figure 3, B and E). These results therefore did not rule out a direct role of one or both RxxL motifs in degron function.

To clarify the significance of individual RxxL motifs for Cdc5(1-80), we created further GFP fusion constructs containing shorter segments of the Cdc5 degron (Figure 4). Cdc5(1-60)-GFP, which lacks the RxxL2 motif but retains the RxxL1 and KEN motifs, was highly unstable in G1 (Figure 4A). Whereas this fusion protein displayed normal levels in nonsynchronized cells (Supplemental Figure S3), the protein failed to accumulate to high levels when expressed in G1-arrested cells and rapidly disappeared after promoter shut-off (Figure 4A). Consistent with this, Cdc5(1-60)-GFP was detected at high levels in the nuclei of mitotic cells but was essentially absent in G1 cells. Mutation of RxxL1 in this construct increased the stability of the fusion protein without causing any detectable mislocalization to the cytoplasm (Figure 4B). Thus, in addition to the essential KEN motif, the RxxL1 motif makes a direct contribution to instability of Cdc5(1-80).

We additionally analyzed a fusion construct comprising amino acids 38–80 of Cdc5 containing only the RxxL2 motif (Figure 4C). This fusion protein was stable in G1 and resided predominantly in

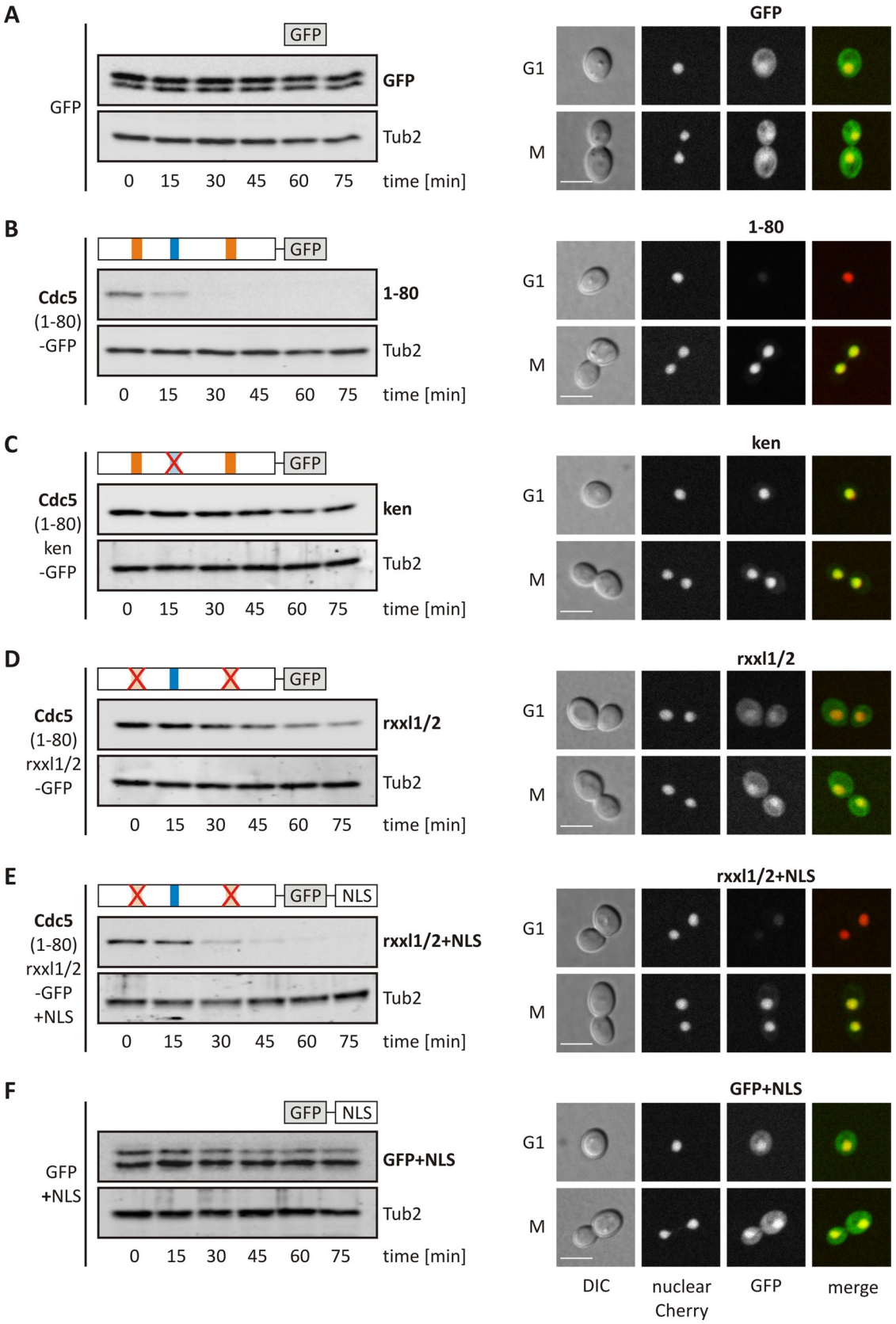

FIGURE 3: The KEN box is an essential motif of the Cdc5 degron. (A–F) Promoter shut-off stability measurements and live-cell imaging of strains expressing (A) GFP, (B) Cdc5(1-80)-GFP, (C) Cdc5(1-80)ken-GFP (ken, K35A/E36A), (D) Cdc5(1-80)rxxl1/2-GFP (rxxl1/2, R17A/L20A/R61A/L64A), (E) Cdc5(1-80)rxxl1/2-GFP+NLS, or (F) GFP+NLS from the regulable *GAL1* promoter. For stability measurements, expression of the constructs was induced for 2 h in cells arrested in G1 by α-factor treatment. After promoter repression by glucose ($t = 0$ min), samples were taken at indicated time

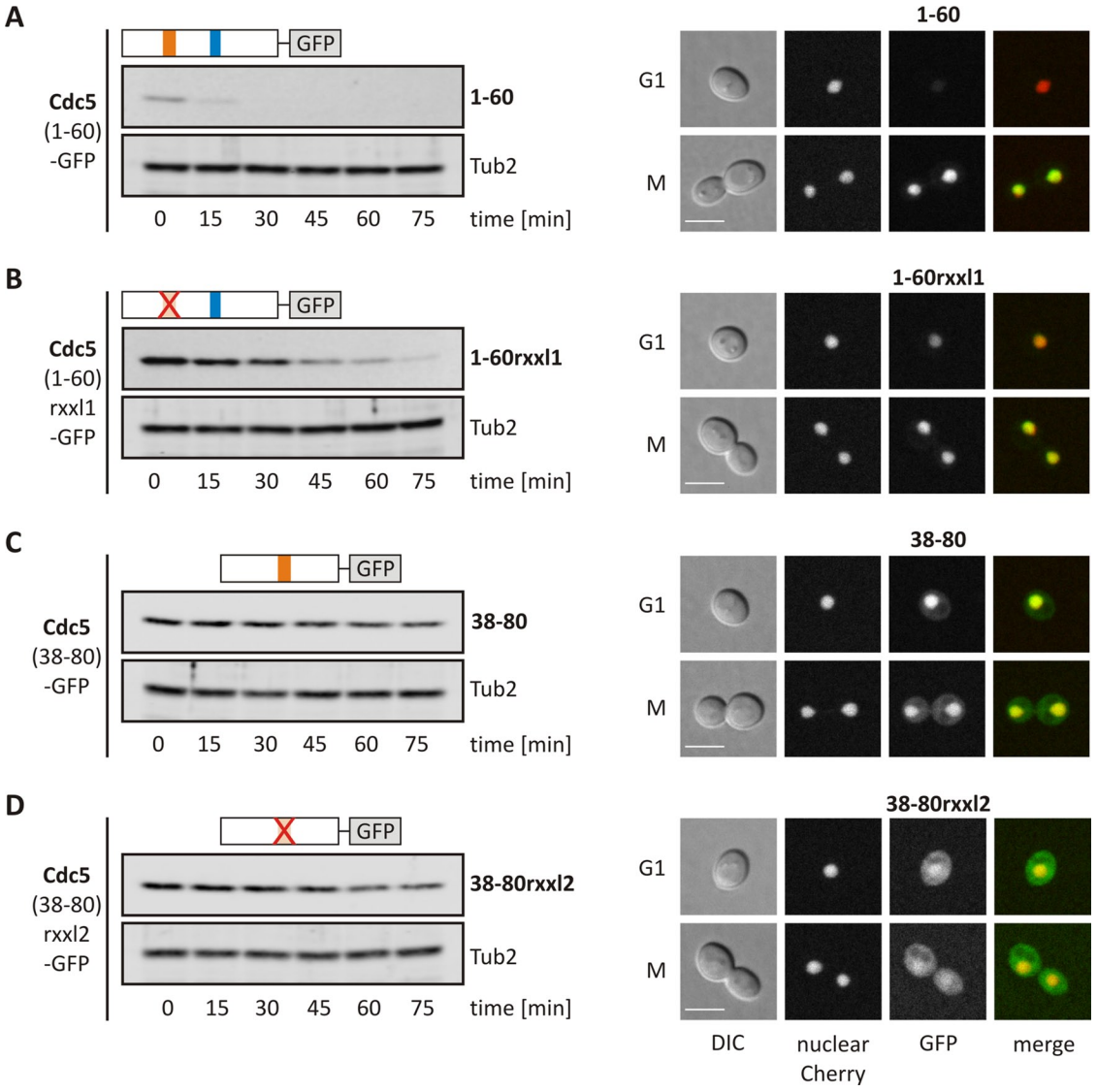

FIGURE 4: RxxL1 is part of the degradation motif of the Cdc5 degron, and RxxL2 is part of an NLS. (A–D) Promoter shut-off stability measurements and live-cell imaging of strains expressing (A) Cdc5(1-60)-GFP, (B) Cdc5(1-60)rxxl1-GFP (rxxl1, R17A/L20A), (C) Cdc5(38-80)-GFP, or (D) Cdc5(38-80)rxxl2-GFP (rxxl2, R61A/L64A) from the regulable *GAL1* promoter as described for Figure 3. Fusion proteins were detected by the Myc-specific antibody 9E10. Tubulin (Tub2), which served as a loading control, was detected by a polyclonal rabbit antiserum. To visualize the nucleus, strains coexpressed a stable nuclear Cherry fusion protein. Representative G1 (top) and mitotic cells (bottom). Merge, merged Cherry and GFP images. Scale bar, 5 μm.

the nucleus (Figure 4C). Of interest, nuclear localization of Cdc5(38-80)-GFP was mostly abolished by mutation of RxxL2 (Figure 4, C and D), indicating that this motif is part of a newly identified NLS in the N-terminal domain of Cdc5.

Taken together, these results indicate that the KEN box is the essential APC/C recognition signal in the Cdc5 degron and is supported by the RxxL1 motif. In contrast, RxxL2 contributes to instability in a distinct manner by promoting nuclear localization.

A single RxxL-type D box is essential for the Cdc20 degron

Yeast Cdc20 contains two RxxL motifs in its N-terminal domain (Figure 1B), and previous work reported that degradation of Cdc20 in G1 depends solely on the first motif (RxxL1, starting at position 17; Prinz *et al.*, 1998; Shirayama *et al.*, 1998). However, more recent data also described a role for the second motif (RxxL2, starting at position 60) for G1-dependent instability of Cdc20 (Robbins and Cross, 2010). To elucidate the individual contributions of both motifs

points and processed for Western analysis. Above the immunoblot images, schematic representations of the respective constructs are shown with mutated sequence elements labeled by red crosses. All constructs were detected by the Myc-specific antibody 9E10. Tubulin (Tub2), detected by a polyclonal rabbit antiserum, served as a loading control. For live-cell imaging, expression of the constructs was induced for 1 h in growing cells, and the cells were then analyzed by confocal fluorescence microscopy. Strains coexpressed a stable nuclear Cherry fusion protein to visualize the nucleus. Representative G1 (top) and mitotic cells (bottom). Merge, merged Cherry and GFP images. Scale bar, 5 μm.

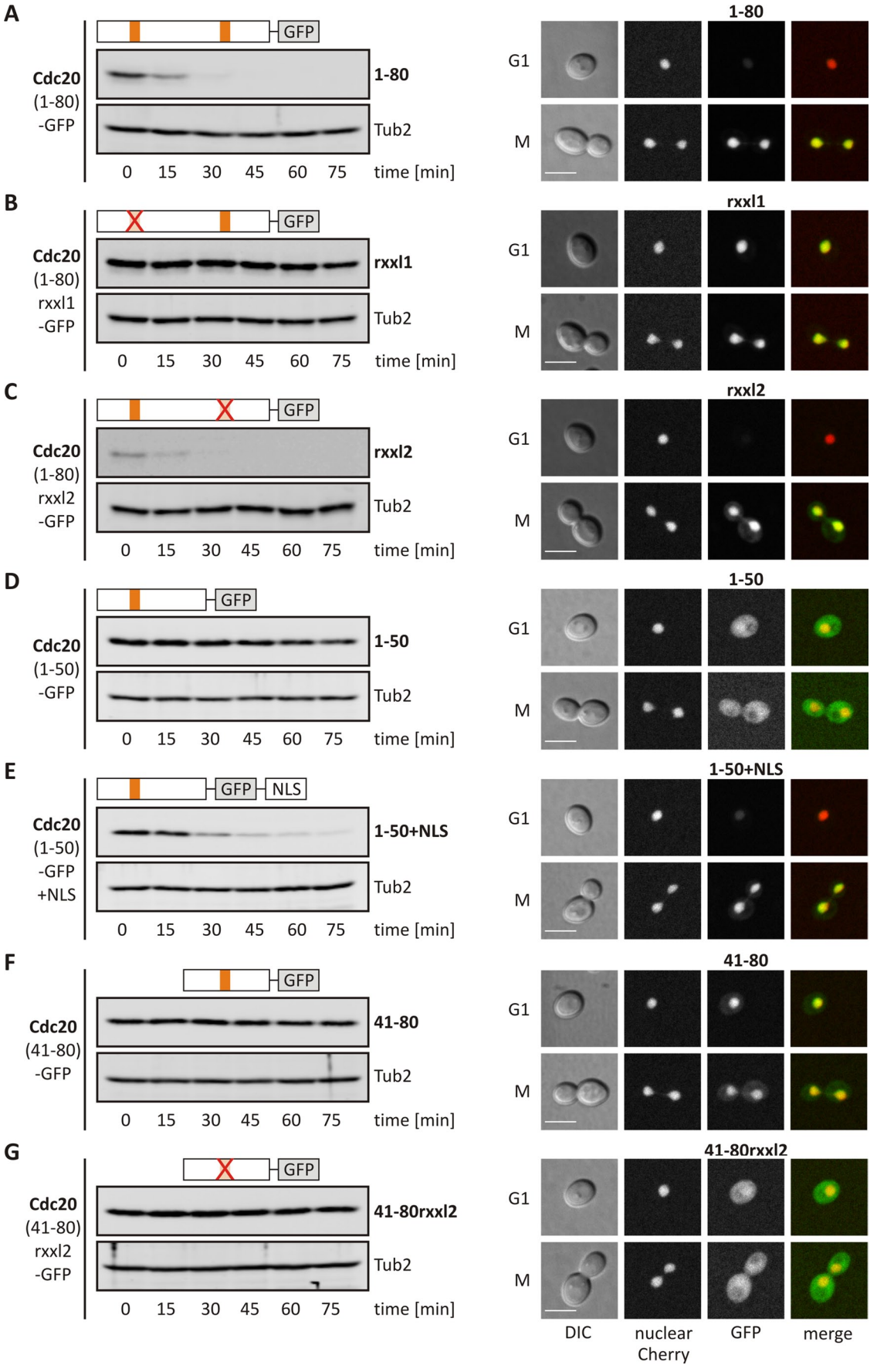
A
Cdc20
(1-80)
-GFP
GFP
1-80
Tub2
0 15 30 45 60 75 time [min]
1-80
G1
M
B
Cdc20
(1-80)
rxxl1
-GFP
GFP
rxxl1
Tub2
0 15 30 45 60 75 time [min]
rxxl1
C
Cdc20
(1-80)
rxxl2
-GFP
GFP
rxxl2
Tub2
0 15 30 45 60 75 time [min]
rxxl2
D
Cdc20
(1-50)
-GFP
GFP
1-50
Tub2
0 15 30 45 60 75 time [min]
1-50
E
Cdc20
(1-50)
-GFP
+NLS
GFP
NLS
1-50+NLS
Tub2
0 15 30 45 60 75 time [min]
1-50+NLS
F
Cdc20
(41-80)
-GFP
GFP
41-80
Tub2
0 15 30 45 60 75 time [min]
41-80
G
Cdc20
(41-80)
rxxl2
-GFP
GFP
41-80rxxl2
Tub2
0 15 30 45 60 75 time [min]
41-80rxxl2
DIC
nuclear
Cherry
GFP
merge

in targeting Cdc20 for degradation, we mutated them separately to AxxA, producing a set of Cdc20(1-80)-GFP constructs, and analyzed the stability of the resulting fusion proteins in G1-arrested cells as described earlier (Figure 5).

The fusion protein containing both RxxL motifs of the Cdc20 degron, Cdc20(1-80)-GFP, showed rapid degradation in G1, which was comparable to Cdc5(1-80)-GFP (Figures 3B and 5A). As a consequence, Cdc20(1-80)-GFP was detectable in the nuclei of mitotic cells but not of unbudded G1 cells (Figure 5A).

Mutation of RxxL1 prevented the degradation of Cdc20(1-80)-GFP (Figure 5B), whereas mutation of RxxL2 failed to stabilize the fusion protein (Figure 5C), indicating that RxxL1 is the crucial APC/C recognition signal for Cdh1-mediated proteolysis of Cdc20. Mutation of neither RxxL1 nor RxxL2 seemed to affect localization of the constructs (Figure 5, B and C). These observations prompted us to generate a shorter segment of the Cdc20 degron comprising amino acids 1–50 to narrow down the minimal degradation sequence of Cdc20. We found that Cdc20(1-50)-GFP, which retained RxxL1 but lacked RxxL2, was rather stable in G1 (Figure 5D). However, this construct resided predominantly in the cytoplasm, raising again the question of whether cytoplasmic localization interfered with instability as already observed for Cdc5(1-80)rxxl1/2-GFP (Figure 3D). We therefore fused the Swi5-derived NLS to the C-terminus of the fusion protein, creating Cdc20(1-50)-GFP+NLS (Figure 5E). Addition of this NLS restored nuclear localization as well as instability of Cdc20(1-50)-GFP. Thus the C-terminal portion of Cdc20(1-80) contributed to Cdh1-dependent degradation by mediating nuclear localization.

Consistent with this notion, amino acids 41–80 of the Cdc20 degron exhibited NLS activity but did not confer G1-dependent instability to GFP (Figure 5F). Mutation of RxxL2 largely prevented nuclear localization of Cdc20(41-80)-GFP (Figure 5G), indicating that the positively charged arginine of RxxL2 is part of a previously unknown NLS. Because mutation of RxxL2 within the longer Cdc20(1-80)-GFP construct had only a minor effect on nuclear localization (Figure 5, C and G), an additional NLS element apparently exists within the N-terminal portion of the Cdc20 degron.

Because the RxxL1 motif was both sufficient and required for degradation of Cdc20(1-80), we conclude that RxxL1 is part of a functional D box that is responsible for targeting of the Cdc20 degron by APC/C-Cdh1. As observed for the Cdc5 degron, nuclear localization turned out to be important for efficient degradation of Cdc20(1-80), and the RxxL2 motif contributed to instability by supporting proper localization to the nucleus. The function of RxxL2 as an NLS element could explain the contradicting results of previous work (Prinz *et al.*, 1998; Shirayama *et al.*, 1998; Robbins and Cross, 2010) regarding the role of RxxL2 for instability of Cdc20.

Target proteins of APC/C-Cdh1 must reside in the nucleoplasm for maximal degradation

Fusion of an NLS to the mutated Cdc5(1-80)rxxl1/2-GFP (Figure 3, D and E) or the truncated Cdc20(1-50)-GFP constructs (Figure 5, D and E) restored not only nuclear localization but also cell cycle–controlled protein instability, suggesting that cytoplasmic localization of a target protein interferes with its APC/C-Cdh1–dependent degradation. If this is indeed the case, targeting of the original Cdc5(1-80)-GFP and Cdc20(1-80)-GFP constructs to the cytoplasm by another means should similarly prevent their degradation.

To address this idea, we fused a nuclear export signal (NES) derived from Nmd3, a protein involved in nuclear export of the large ribosomal subunit (Gadal *et al.*, 2001), to the C-termini of Cdc5(1-80)-GFP and Cdc20(1-80)-GFP. The resulting constructs, Cdc5(1-80)-GFP+NES and Cdc20(1-80)-GFP+NES, localized to the cytoplasm and were excluded from the nucleus (Figure 6A). This indicated that the effect of the NES was dominant over the native NLS present in the Cdc5 and Cdc20 degrons. In fact, the nucleus-excluded Cdc5 and Cdc20 degron constructs were barely degraded in G1 (Figure 6A). Proteolysis was not affected by C-terminal fusion of an NLS to Cdc5(1-80)-GFP and Cdc20(1-80)-GFP (Figure 6B), arguing against a general stabilizing effect through manipulation of these constructs at their C-termini. Thus these findings confirm the idea that APC/C-Cdh1–dependent degradation is confined to the nucleus.

Increased stability through cytoplasmic localization was also observed for full-length Cdc5 (Supplemental Figure S6). Fusion of an NLS or NES to Cdc5-GFP brought about the expected differential localization to the nucleus or cytoplasm, respectively. When expressed in nonsynchronized cells, both constructs accumulated to similar levels. In G1 cells, however, the cytoplasmic Cdc5-GFP+NES version accumulated to higher levels and turned over more slowly than the nuclear Cdc5-GFP+NLS construct. These results substantiate the relevance of substrate localization for proteolysis by the APC/C-Cdh1 pathway.

In previous studies, the APC/C was described to localize to the kinetochore and chromatin in both yeast and mammalian cells (Topper *et al.*, 2002; Melloy and Holloway, 2004). We therefore asked whether there are differences in APC/C-Cdh1 activity within different subcompartments of the nucleus, and we created additional constructs to address this question (Figure 7). We first fused the histones H1 and H2B to Cdc5(1-80)-GFP and Cdc20(1-80)-GFP to link the resulting fusion proteins to chromatin. Whereas the histone H1 fusions were distributed over the nucleus and colocalized with the nuclear Cherry marker, the histone H2B fusions colocalized with H2A-yEmRFP in a more compact nuclear structure (Supplemental Figure S7), consistent with incorporation of H2B fusions into nucleosomes and loose chromatin association of H1 constructs (Figure 7, A and B). Promoter shut-off stability measurements indicated that fusions of the Cdc5 and Cdc20 degrons to histone H1 resulted in little or no stabilization, whereas fusions to histone H2B caused a moderate reduction of protein turnover (Figure 7, A and B). Thus localization to chromatin did not alter the degradation kinetics of Cdc5 and Cdc20 degron constructs, suggesting that APC/C-Cdh1 activity is not enriched on chromatin in budding yeast. Instead, localization to the nucleosomal core seems to reduce the efficiency of APC/C-Cdh1–dependent degradation.

FIGURE 5: RxxL1 of the Cdc20 degron is a functional D box, and RxxL2 is part of an NLS. (A–G) Promoter shut-off stability measurements and live-cell imaging of strains expressing (A) Cdc20(1-80)-GFP, (B) Cdc20(1-80)rxxl1-GFP (rxxl1, R17A/L20A), (C) Cdc20(1-80)rxxl2-GFP (rxxl2, R60A/L63A), (D) Cdc20(1-50)-GFP, (E) Cdc20(1-50)-GFP+NLS, (F) Cdc20(41-80)-GFP, or (G) Cdc20(41-80)rxxl2-GFP from the regulable *GAL1* promoter as described for Figure 3. Fusion proteins were detected by the Myc-specific antibody 9E10. Tubulin (Tub2), which served as a loading control, was detected by a polyclonal rabbit antiserum. To visualize the nucleus, strains coexpressed a shown. Merge, merged Cherry and GFP images. Scale bar, 5 μm.

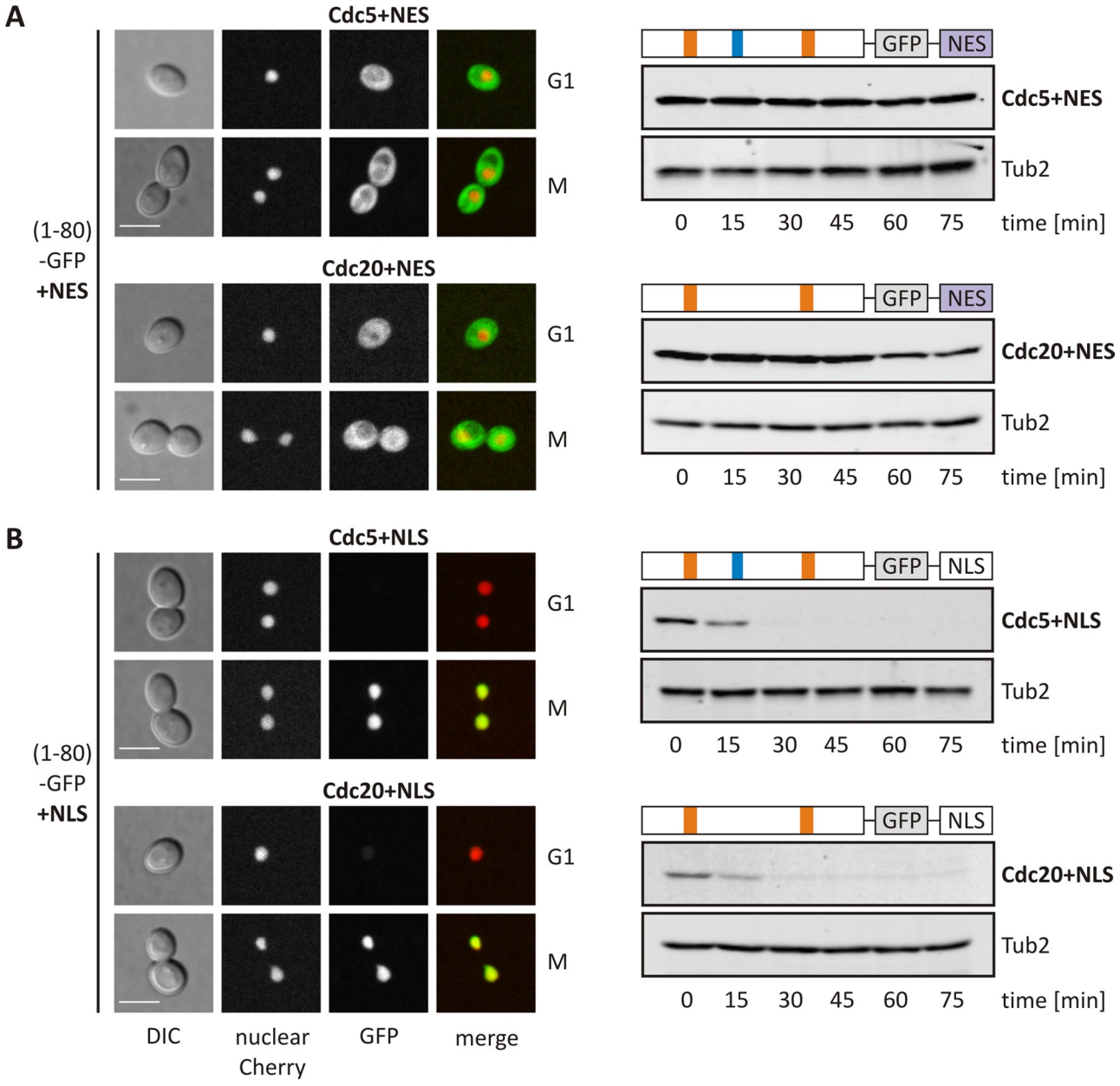

FIGURE 6: Nuclear localization is required for KEN and D box–mediated degradation in G1. Live-cell imaging and promoter shut-off stability measurements of strains expressing (A) Cdc5(1-80)-GFP+NES or Cdc20(1-80)-GFP+NES and (B) Cdc5(1-80)-GFP+NLS or Cdc20(1-80)-GFP-NLS from the regulable *GAL1* promoter as described for Figure 3. To visualize the nucleus, strains coexpressed a stable nuclear Cherry fusion protein. Representative G1 (top) and mitotic cells (bottom). Merge, merged Cherry and GFP images. Scale bar, 5 μm. Fusion proteins were detected by the Myc-specific antibody 9E10. Tubulin (Tub2), which served as a loading control, was detected by a polyclonal rabbit antiserum.

We also fused Cdc5(1-80)-GFP and Cdc20(1-80)-GFP to the rDNA-binding protein Hmo1 to target the degron constructs to the nucleolus (Figure 7C). The resulting fusion proteins colocalized with the nucleolar marker protein Nop56-3mCherry, indicating that the Hmo1-fusions indeed resided predominantly in the nucleolus (Figure 7C). In contrast to the original Cdc5(1-80)-GFP and Cdc20(1-80)-GFP constructs, the Hmo1 fusion proteins were still detectable in G1 cells, although their signals were less intense than in mitotic cells. In agreement with this observation, protein stability measurements indicated that the degradation of Cdc5(1-80)-GFP+Hmo1 and Cdc20(1-80)-GFP+Hmo1 was reduced compared with Cdc5(1-80)-GFP and Cdc20(1-80)-GFP (Figures 3B, 5A, and 7C). Thus targeting of the Cdc5(1-80)-GFP and Cdc20(1-80)-GFP to the nucleolus by Hmo1 rendered these proteins less accessible for proteolysis by APC/C-Cdh1.

Taken together, these findings indicate that nucleus-localized target proteins are most accessible for APC/C-Cdh1–mediated degradation when they reside in the nucleoplasm.

Subcellular localization of substrates may affect the timing of their degradation

Our analysis of KEN and D box degron constructs indicated that Cdh1 substrates are protected from degradation as long as they

reside in the cytoplasm (Figures 3D, 5D, and 6A and Supplemental Figure S6B), arguing that APC/C-Cdh1 function in budding yeast is restricted to the nucleus. This spatial confinement opens up the opportunity for temporal control of APC/C-Cdh1–mediated proteolysis, since certain cytoplasmic Cdh1 substrates may enter the nucleus only after APC/C-Cdh1 activation. To test whether subcellular localization may affect the timing of proteolysis, we chose to compare the degradation onsets of Ase1, a nuclear substrate of Cdh1 (Juang *et al.*, 1997), and Iqg1, a Cdh1 substrate that localizes outside the nucleus (Ko *et al.*, 2007). Whereas the microtubule-associated protein Ase1 localizes to the spindle midzone to control assembly and elongation of the mitotic spindle (Winey and Bloom, 2012), Iqg1 is involved in actin–myosin ring assembly and is recruited to the bud neck during mitosis (Shannon, 2012). To follow Ase1 and Iqg1 in living cells, we integrated the GFP gene at the 3′ end of the endogenous *ASE1* and *IQG1* genes, creating C-terminal GFP fusion proteins expressed from their native promoters. In addition, we tagged endogenous *CDC14* with GFP to visualize the release of Cdc14 phosphatase from the nucleolus into the cytoplasm and its known subsequent localization to the spindle pole body (SPB) entering the daughter cell (dSPB; Yoshida *et al.*, 2002). Because Cdc14 is responsible for removal of the inhibitory phosphorylation of Cdh1 in budding yeast (Visintin *et al.*, 1998; Jaspersen *et al.*, 1999), we used Cdc14 release to estimate the timing of Cdh1 activation.

We found that Cdc14-GFP was released from the nucleolus and appeared at the dSPB 16.5 min (± 4 min; $n = 10$) before spindle breakdown and returned to the nucleolus shortly after the spindle had collapsed (Figure 8, A and D, and Supplemental Movie 8A). Consistent with the requirement of Cdc14 for activation of Cdh1, degradation of both Ase1-GFP and Iqg1-GFP showed a delay relative to the release of Cdc14 (Figure 8D). Ase1-GFP was first detectable after SPB duplication and persisted at the spindle midzone during elongation of the mitotic spindle (Figure 8B and Supplemental Movie 8B). The signal intensity of Ase1-GFP then started to decrease 7 min (±3 min; $n = 10$) before breakdown of the spindle (Figure 8D). Unlike Ase1-GFP, Iqg1-GFP was first detectable during late anaphase, when the protein accumulated at the bud neck (Figure 8C and Supplemental Movie 8C). Recruitment of Iqg1-GFP to the bud neck was still in progress at a time when Ase1-GFP degradation had already begun. The signal of Iqg1-GFP finally started to contract at the time of spindle breakdown (0 ± 1 min; $n = 10$) and disappeared subsequently (Figure 8, C and D, and Supplemental Movie 8C). Thus degradation of the bud neck-associated, cytoplasmic protein Iqg1 started with a distinct delay relative to the spindle-associated, nuclear protein Ase1. These data suggest that the degradation onset of a cytoplasmic protein may be uncoupled temporally from Cdh1 activation. Instead of Cdh1 activation in the nucleus, mechanisms controlling entry of the target protein into the nucleus may define the onset of proteolysis in case of a nonnuclear Cdh1 substrate.

DISCUSSION

This study reports that small, N-terminal segments of the yeast polo kinase Cdc5 or the APC/C activator Cdc20 are potent degrons capable of targeting fusion proteins for rapid, cell cycle–controlled proteolysis mediated by the ubiquitin ligase APC/C. Analysis of their composition revealed an essential KEN box in the Cdc5-derived sequence, whereas a D box was the required degradation signal in the Cdc20(1-80) element (Figures 3 and 5). Despite the presence of these canonical APC/C recognition motifs, neither degron was degraded in the absence of Cdh1 (Figure 2 and Supplemental Figure S2), indicating that these degrons are specific for Cdh1 and cannot be targeted by Cdc20. This was surprising, given the fact that the receptor sites for D and KEN boxes are highly conserved among the APC/C activator paralogues Cdc20 and Cdh1 (Chao, Kulkarni *et al.*, 2012; Tian, Li, *et al.*, 2012; He *et al.*, 2013). Therefore one might have expected that degrons containing a KEN or D box would be recognized by Cdc20 as well. One possible explanation would be that both degrons, despite their short lengths, contain additional and as-yet-unidentified sequence elements that confer specificity for binding to Cdh1. This idea is supported by a crystal structure displaying the WD40 domain of Cdh1 bound to a 70–amino acid fragment of its inhibitor, Acm1 (He *et al.*, 2013). Comparable to the Cdc5 and Cdc20 degrons, the central inhibitory region (CIR) of Acm1 carries D and KEN box motifs that occupy the corresponding receptor sites on the WD40 domain of Cdh1. In addition, the CIR contains the so-called A motif (EETAE; Burton *et al.*, 2011), which was reported to contact a binding site on the Cdh1-WD40 domain that is not conserved in Cdc20 (He *et al.*, 2013) and is therefore believed to mediate Cdh1-specific binding of the inhibitor. However, the degrons analyzed in this study do not exhibit any motifs that resemble the A motif of Acm1, nor do the degrons themselves share any similar sequence elements among each other, except for the RxxL motifs. Perhaps sequence motifs for Cdh1 specificity are variable among substrates, and the WD40 domain of Cdh1 provides multiple distinct contact sites. Specific requirements of Cdc20 for proper substrate binding involving interaction motifs in addition to D and KEN boxes would be another possible explanation. Following this idea, Cdc20 would recognize a limited set of substrates that meet its stringent requirements, whereas Cdh1 represents a more diversified activator of the APC/C. This model would fit the known roles for Cdc20 and Cdh1 during mitosis. Cdc20 is mainly required to remove securin and initiate degradation of cyclins to trigger anaphase onset. In contrast, Cdh1 is later responsible for the degradation of many different proteins that must not be degraded until all mitotic events are executed (Peters, 2006; Primorac and Musacchio, 2013).

The spatial arrangement of the D and KEN box receptor sites on the WD40 propeller domain of the APC/C activators suggested cooperative binding of a substrate carrying suitably positioned D and KEN boxes (Chao, Kulkarni, *et al.*, 2012). Even though both motifs were found in the Cdc5 degron, cooperativity might not be involved, since the D box precedes the KEN box, which is inconsistent with the proposed orientation, and had only a moderate share in instability, whereas the KEN box was essentially indispensable. Moreover, in case of the Cdc20 degron, a single D box as the only detectable APC/C recognition motif supported rapid degradation (Figure 2). Thus cooperative binding of APC/C recognition motifs is not a general requirement for efficient in vivo proteolysis of an APC/C substrate.

In addition to an APC/C recognition motif, an NLS was found to be an essential part of the Cdc5- and Cdc20-derived in vivo degrons. In both cases, the NLS resided C-terminal to the identified APC/C recognition motif as a discrete functional element (Figures 4C and 5F) and incorporated an RxxL motif whose mutation abolished NLS activity (Figures 4D and 5G). This degron structure resembles a previously described degradation domain identified at the C-terminal end of the spindle motor protein Cin8 (Hildebrandt and Hoyt, 2001). The Cin8 degron was shown to be sufficient for APC/C-Cdh1–dependent degradation and contains a KEN box followed by an NLS that was required for instability and contained an RxxL motif. However, a heterologous NLS lacking RxxL motifs reversed protein stabilization caused by deletion or mutation of the native NLS both in our (Figures 3E and 5E) and the

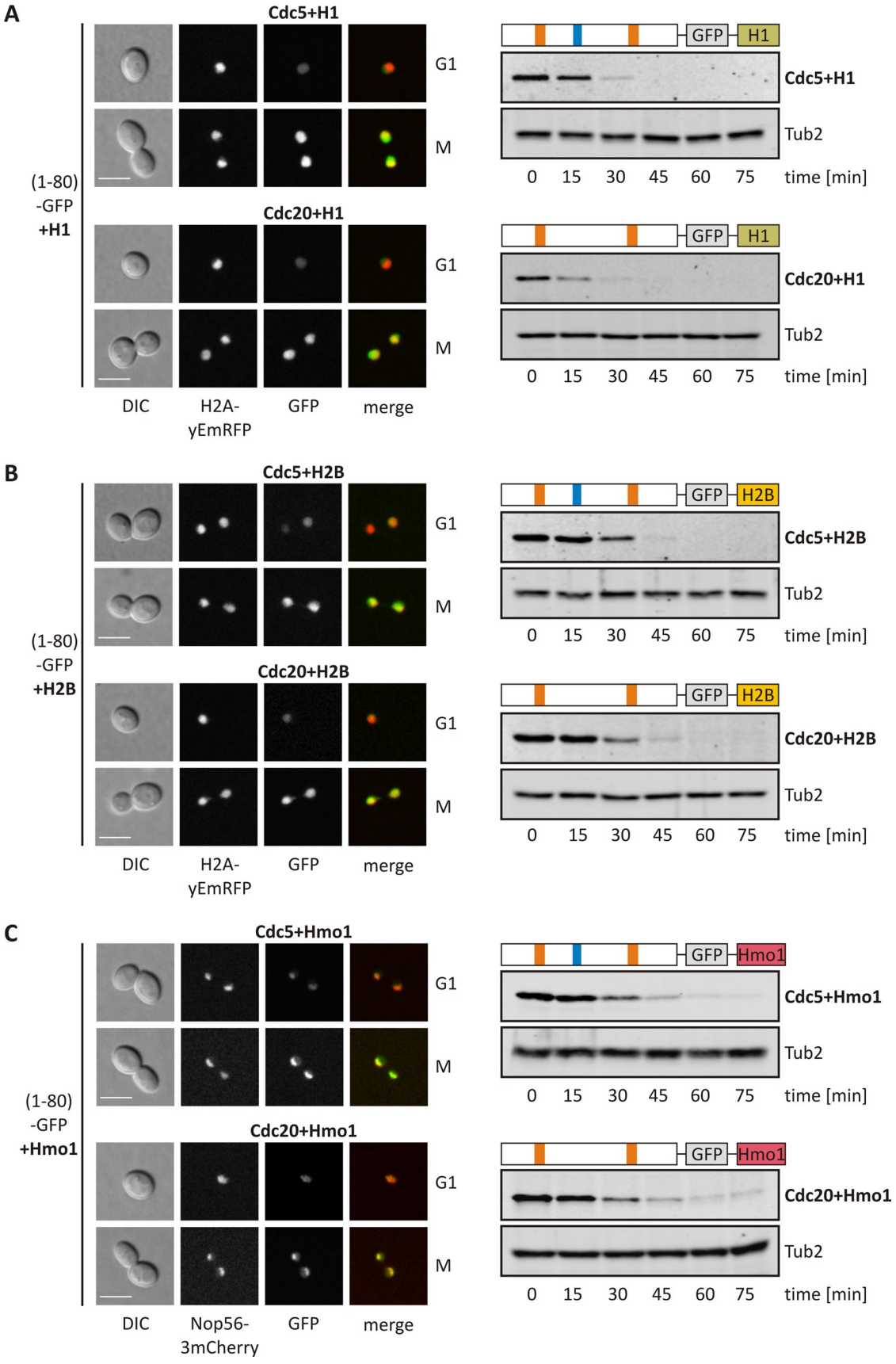

FIGURE 7: Localization to chromatin or the nucleolus delays degradation of Cdc5(1-80)-GFP and Cdc20(1-80)-GFP in G1. Live-cell imaging and promoter shut-off stability measurements of strains expressing (A) Cdc5(1-80)-GFP+H1 or Cdc20(1-80)-GFP+H1, (B) Cdc5(1-80)-GFP+H2B or Cdc20(1-80)-GFP+H2B, and (C) Cdc5(1-80)-GFP+Hmo1 or Cdc20(1-80)-GFP+Hmo1 from the regulable *GAL1* promoter as described for Figure 3. To visualize chromatin or the

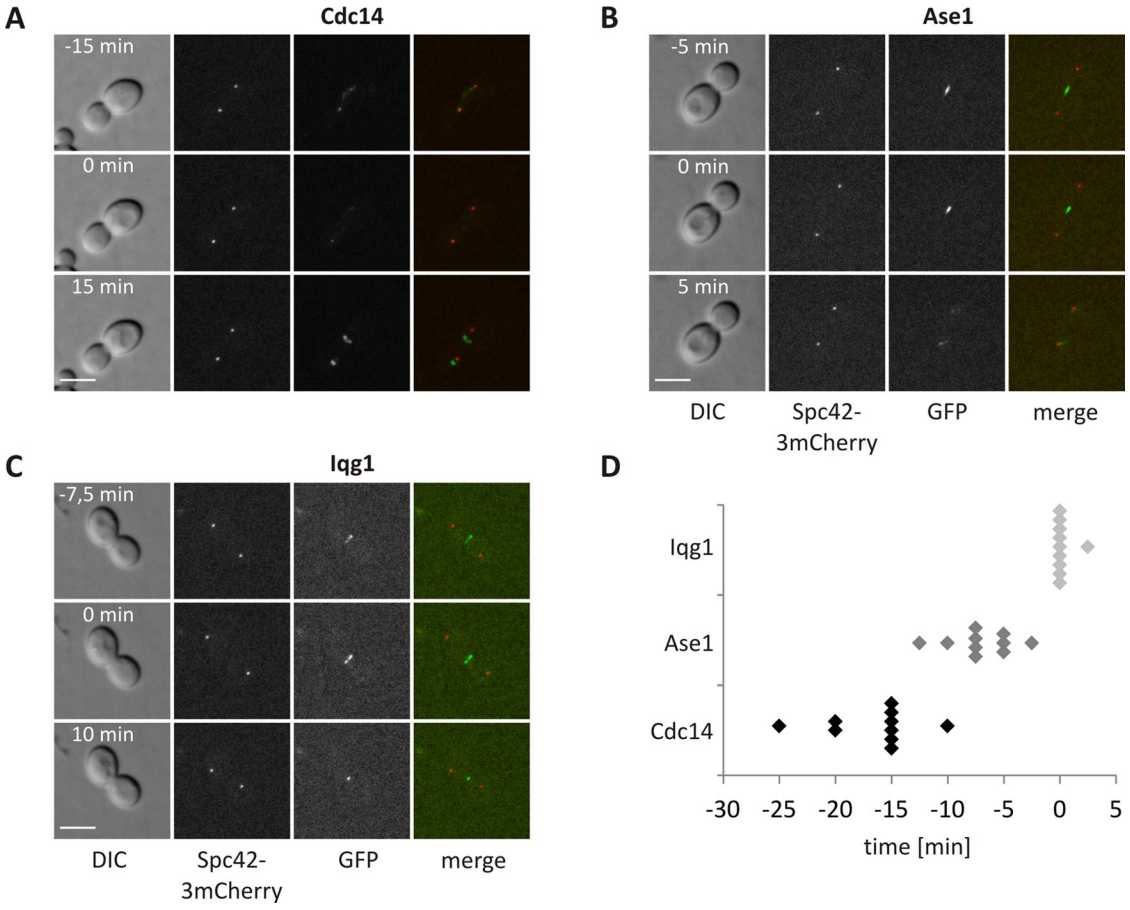

FIGURE 8: Timing of degradation of a nuclear and a cytoplasmic Cdh1 substrate. Cell cycle–dependent localization of (A) Cdc14-GFP, (B) Ase1-GFP, and (C) Iqg1-GFP were followed by live-cell imaging. Strains coexpressed Spc42-3mCherry to visualize SPBs. Spindle breakdown was set to $t = 0$ min and was defined as the maximum distance between the SPBs. Selected time frames of movies (Supplemental Movies 8A–8C) are shown. Merge, merged Cherry and GFP images. Scale bar, 5 μm. (D) To determine the onset of Ase1-GFP (dark gray rhombs) and Iqg1-GFP (light gray rhombs) degradation, the signal intensities were measured in 2.5-min intervals and quantified. The time frame of maximum signal intensity or maximum signal length was used to define the onset of Ase1-GFP or Iqg1-GFP degradation, respectively. The appearance of Cdc14-GFP (black rhombs) at the dSPB was used to define the release of Cdc14-GFP from the nucleolus (5-min intervals). For each strain, 10 cells were quantified.

Cin8 (Hildebrandt and Hoyt, 2001) experiments. This argues that an NLS as such is critical for APC/C-Cdh1–dependent degradation but not the sequence of the NLS per se. Instead, the similar overall composition, the presence of an RxxL motif containing NLS, and the location of the degrons at the extreme ends of their native proteins may suggest that these degrons evolved from a common autonomous precursor module that associated with different proteins during evolution to allow control of their abundance by APC/C-Cdh1.

Previous work in budding yeast, including localization of the APC/C to the nucleus (Zachariae, Shin, *et al.*, 1996; Melloy and Holloway, 2004), a possible link between nuclear localization and Cdh1 function (Jaquenoud *et al.*, 2002), and the analysis of Cin8 degradation (Hildebrandt and Hoyt, 2001), already pointed to the nucleus as the primary compartment for APC/C-Cdh1–dependent proteolysis. Our results strengthen this view. We found that mislocalization to the cytoplasm interfered with rapid proteolysis of D and KEN box degron constructs (Figures 3D and 5D), and retargeting of the constructs to the nucleus by fusion of a heterologous NLS restored their rapid degradation (Figures 3E and 5E). Moreover, forcing the degron constructs to the cytoplasm by an efficient NES minimized their degradation and rendered them virtually stable (Figure 6A). Together these data argue that in budding yeast, the APC/C-Cdh1 proteolysis pathway is essentially restricted to the nucleus. Whether localization of the APC/C or Cdh1 is the determining factor for nuclear degradation is a question for future research.

Nuclear compartmentalization of APC/C-Cdh1 function raises the question of how cytoplasmic substrates, such as the yeast proteins Hsl1 and Iqg1 (Burton and Solomon, 2000; Ko *et al.*, 2007), are targeted by this proteolysis pathway. We observed that levels of Cdc5(1-80)-GFP+NES, Cdc20(1-80)-GFP+NES, and Cdc5(1-80)

nucleolus, strains coexpressed the histone fusion H2A-yEmRFP or the nucleolar marker Nop56-3mCherry. Representative G1 (top) and mitotic cells (bottom). Merge, merged Cherry and GFP images. Scale bar, 5 μm. Fusion proteins were detected by the Myc-specific antibody (9E10), and tubulin (Tub2), which served as a loading control, was detected by a polyclonal rabbit antiserum.

rxxl1/2-GFP, which carried functional D or KEN box recognition motifs and localized to the cytoplasm, barely changed during the cell cycle phase when Iqg1 was degraded (Figures 3D, 6A, and 8C), arguing against the existence of cytoplasmic APC/C-Cdh1 activity. We therefore propose that cytoplasmic substrates, such as Iqg1, have to be imported into the nucleus for their APC/C-Cdh1–mediated degradation. We envisage that Iqg1 is liberated from the bud neck during actin–myosin ring contraction and targeted into the nucleus through an intrinsic NLS for its proteolysis. A nuclear import requirement for cytoplasmic substrates is also consistent with previous work, which suggested that yeast Hsl1 is ubiquitinated by nuclear Cdh1 (Jaquenoud *et al.*, 2002).

The confinement of APC/C-Cdh1–mediated degradation to the nucleus may serve as a cellular mechanism for ordering the degradation of substrates according to their subcellular localization. Indeed, we found that a cytoplasmic Cdh1 substrate, Iqg1, was degraded detectably later than the nuclear substrate Ase1 (Figure 8). Thus, in addition to the known cell cycle–controlled activation of APC/C-Cdh1 (Morgan, 1999; Peters, 2006), which generates nuclear Cdh1 activity, temporal control of this proteolytic pathway may also occur at the level of cytoplasmic substrates. This spatiotemporal mechanism for the control of Cdh1-mediated proteolysis may be conserved among eukaryotes, since the APC/C and Cdh1 were reported to localize to the nucleus in mammalian cells (Jörgensen *et al.*, 1998; Gieffers *et al.*, 1999; Topper *et al.*, 2002; Zhou *et al.*, 2003), and degradation of human Skp2 by the APC/C-Cdh1 pathway required Skp2 nuclear import, which was controlled by transforming growth factor β signaling (Hu, Liu, *et al.*, 2011). In fact, substrate-level control of Cdh1-dependent proteolysis may even be more widespread in metazoan organisms, in which the APC/C-Cdh1 ubiquitin ligase functions in nonmitotic processes such as metabolism, cell differentiation, and survival (Gieffers *et al.*, 1999; Eguren *et al.*, 2011; Almeida, 2012).

MATERIALS AND METHODS

Yeast methods

Standard protocols were followed for transformation, mating, sporulation, and tetrad dissection of yeast cells (Ausubel *et al.*, 2005). Yeast strains used in this study are derivatives of W303 and listed in Supplemental Table S1. Cells were grown at 25°C in yeast extract/peptone (YEP) complex medium containing adenine (100 mg/l), tryptophan (200 mg/l), and KH_2PO_4 (10 mM) supplemented with 2% glucose or 2% raffinose. Expression from the *GAL1* promoter was induced by addition of 2% galactose to cells grown in medium containing raffinose. For repression of the *GAL1* promoter, cells were harvested by centrifugation and released into fresh YEP complex medium with 2% glucose. For cell cycle synchronization, cells were arrested in G1 phase by pheromone treatment (50 ng/ml α-factor).

DNA constructs and genetic manipulations

Genes were amplified by PCR from yeast genomic DNA (W303 or S288C). PCR primers contained restriction sites for subsequent cloning. All PCR-amplified constructs were verified by commercial DNA sequencing (Seqlab, Göttingen, Germany). Yeast plasmid constructs used in this study are derivatives of pRS vectors (Sikorski and Hieter, 1989) and listed in Supplemental Table S2.

A codon-optimized version of the GFP gene was used (Cormack *et al.*, 1997). Codons 1–80 of *CDC5* and *CDC20*, as well as their derivatives, were cloned into pWS2741 (*pGAL1-MYC3-GFP-tCYC1*). *CDC5*(codons1-80)-GFP and *CDC20*(codons1-80) were cloned into pWS3232 (*pTEF2-MYC3-tCYC1*) and pWS3351 (*pTEF2-MYC3-GFP-tCYC1*), respectively. To delete the RxxL motifs or the KEN box of *CDC5* and *CDC20*, the conserved arginine and leucine codons (RxxL; Figure 1, A and B) or lysine and glutamate codons (KEN; Figure 1A) were replaced by alanine codons, respectively, using site-directed mutagenesis (Stratagene, La Jolla, CA). *CDC5*(codons1-80) rxxl1/2 was amplified using pJC88 (Charles *et al.*, 1998) as a template.

CDC14(codons183-551) and *NOP56*(codons318-504) were amplified from yeast genomic DNA (S288C) and cloned into pRS vectors including the GFP gene (*CDC14*(codons183-551)-*GFP-tCYC1*) or 3mCherry (Shaner *et al.*, 2004; *NOP56*(codons318-504)-*3mCherry-tCYC1*), respectively, and the resulting constructs were integrated at the respective gene loci. *SPC42* was amplified together with its endogenous promoter from yeast genomic DNA (S288C) and cloned into a pRS vector including 3mCherry (*pSPC42-SPC42-3mCherry-tCYC1*), and the resulting construct was integrated at the *TRP1* locus. For deletion of *BAR1*, the corresponding deletion cassette was amplified from yeast genomic DNA (EUROSCARF, Frankfurt, Germany) and integrated at the *BAR1* locus. GFP gene fusions of endogenous *ASE1* and *IQG1*, as well as a yEmRFP gene fusion of endogenous *HTA2*, were constructed by PCR-based epitope tagging as described (Sheff and Thorn, 2004). The pFA6a-link-yEmRFP plasmid was generated by replacing the GFP gene of pKT128 (Sheff and Thorn, 2004) vector with the yEmRFP gene, which was amplified from yEp-GAP-yEmRFP plasmid (Keppler-Ross *et al.*, 2010).

To visualize the nucleus, a construct named nuclear Cherry was integrated at the *URA3* or *TRP1* locus. Nuclear Cherry consists of the mCherry gene fused to codons 569–709 of *SWI5* (Moll *et al.*, 1991), followed by a *MYC13* tag and *tCYC1*. The *SWI5* fragment contained point mutations at codons 646 and 664 replacing serine by alanine codons at two Cdk1 sites to provide constitutive nuclear localization. This construct was placed under the control of the constitutive *TEF2* promoter (*pTEF2-mCherry-SWI5*(codons569-709) S646A/S664A-*MYC13-tCYC1*; Supplemental Table S2).

Codons 614–663 of *SWI5* with a single point mutation S646A served as NLS (Supplemental Table S2; Moll *et al.*, 1991) and codons 441–518 of *NMD3* as NES (Supplemental Table S2; Gadal *et al.*, 2001).

Protein analysis

For preparation of yeast protein extracts, cells were harvested by centrifugation and washed once with ice-cold H_2O. Lysis buffer (150 mM NaCl, 50 mM Tris-HCl, pH 7.5, 50 mM NaF, 5 mM EDTA, 0.1% IGEPAL CA-630, 60 mM β-glycerol phosphate) was added, and the cell suspension was shaken with an equal volume of glass beads in a mixer mill (Retsch, Haan, Germany) for 5 min at 4°C. After removal of cell debris by centrifugation at 4°C, equal volumes of supernatant and 2× Laemmli sample buffer were mixed and incubated for 10 min at 100°C.

SDS–PAGE and Western analysis were performed as described (Schwab *et al.*, 1997, 2001). Mouse monoclonal antibody 9E10 and mouse monoclonal anti-GFP antibody (Roche, Basel, Switzerland) were used for detection of Myc-tagged proteins and Cdc20(1-80)-GFP fusion protein (Figure 1G), respectively. Gcd11 was detected using affinity-purified polyclonal rabbit antiserum (Perzlmaier, Richter, *et al.*, 2013). Tub2 and Clb2 were probed by specific polyclonal rabbit antisera. Immunoblots were detected with an Odyssey Infrared Imaging System (LI-COR Biosciences, Bad Homburg, Germany) using goat anti-mouse IRDye 800 and goat anti-rabbit IRDye 680 as secondary antibodies (LI-COR Biosciences).

Fluorescence microscopy

To determine bud formation and nuclear division, ethanol-fixed cells were washed and resuspended in sodium citrate (50 mM, pH 7.0). After sonification, DNA was stained by 4′,6-diamidino-2-phenylindole (DAPI; Sigma-Aldrich, St. Louis, MO). Cells were analyzed using an Axio Imager microscope (Carl Zeiss, Jena, Germany) equipped with an AxioCam MRm camera (Carl Zeiss).

For live-cell imaging, exponentially growing cells were harvested by centrifugation and covered with agarose supplied with yeast nitrogen base, amino acids, and 2% glucose (for imaging of *TEF2* promoter constructs) or 2% raffinose/1% galactose (for imaging of *GAL1* promoter constructs). Expression of GFP fusion constructs from the *GAL1* promoter was induced by addition of 2% galactose for 60 min at 25°C before microscopy. Cells were observed using a Plan Apochromat 63×/1.40 oil differential interference contrast (DIC) M27 lens on an Observer Z.1 confocal spinning disk (CSU-X1) microscope (Yokogawa, Tokyo, Japan; Carl Zeiss) at 20–22°C. Ten *z*-planes at 0.5-µm distance were taken with a shutter speed of 200 ms using an AxioCam MRm camera (Carl Zeiss). For time-lapse images shown in Figures 2 and 8A as well as in corresponding supplemental movies, *z*-stacks were taken every 5 min. For Figure 8, B and C, as well as for corresponding supplemental movies, *z*-stacks were taken every 2.5 min. Microscopy data were processed and quantified using ImageJ (National Institutes of Health, Bethesda, MD). To prepare images, *z*-stacks of the region of interest were projected using median-intensity projection (DIC channel) or maximum-intensity projection (fluorescence channels). For quantifications shown in Figures 2 and 8 and Supplemental Figure S2, total fluorescence was measured for every time point after summation of *z*-planes and subtraction of background. An area without cells or fluorescent objects was used for background subtraction. The fluorescence intensity was measured using threshold settings. For Figure 2 and Supplemental Figure S2, raw integrated density was plotted against the time axis.

Flow cytometry

To measure the DNA content, flow cytometry was done essentially as described (Geil *et al.*, 2008) with a CyFlow Space cytometer (Partec, Münster, Germany). For every sample, the DNA content of 20,000 cells was measured, and resulting data were analyzed with the WinMDI 2.8 software.

ACKNOWLEDGMENTS

We thank Andrea Brücher, Antje Machetanz-Morokane, and Adelheid Weissgerber for technical assistance; Frank Sprenger for help with microscopy; Wolfgang Mages for comments on the manuscript; David Morgan (University of California, San Francisco, San Francisco, CA) for plasmid pJC88; and Neta Dean (Stony Brook University, Stony Brook, NY) for a yEmRFP plasmid. S.H. was supported by a PhD fellowship from the Elitenetzwerk Bayern.

REFERENCES

Boldface names denote co–first authors.

Almeida A (2012). Regulation of APC/C-Cdh1 and its function in neuronal survival. Mol Neurobiol 46, 547–554.

Ausubel FM, Brent R, Kingston RE, Moore DD, Seidman JG, Smith JA, Struhl K (2005). Current Protocols in Molecular Biology, New York: John Wiley & Sons.

Barford D (2011). Structural insights into anaphase-promoting complex function and mechanism. Philos Trans R Soc Lond B Biol Sci 366, 3605–3624.

Barral Y, Parra M, Bidlingmaier S, Snyder M (1999). Nim1-related kinases coordinate cell cycle progression with the organization of the peripheral cytoskeleton in yeast. Genes Dev 13, 176–187.

Burton JL, Solomon MJ (2000). Hsl1p, a Swe1p inhibitor, is degraded via the anaphase-promoting complex. Mol Cell Biol 20, 4614–4625.

Burton JL, Solomon MJ (2001). D box and KEN box motifs in budding yeast Hsl1p are required for APC-mediated degradation and direct binding to Cdc20p and Cdh1p. Genes Dev 15, 2381–2395.

Burton JL, Xiong Y, Solomon MJ (2011). Mechanisms of pseudosubstrate inhibition of the anaphase promoting complex by Acm1. EMBO J 30, 1818–1829.

Bäumer M, Kunzler M, Steigemann P, Braus GH, Irniger S (2000). Yeast Ran-binding protein Yrb1p is required for efficient proteolysis of cell cycle regulatory proteins Pds1p and Sic1p. J Biol Chem 275, 38929–38937.

Chao WC, Kulkarni K, Zhang Z, Kong EH, Barford D (2012). Structure of the mitotic checkpoint complex. Nature 484, 208–213.

Charles JF, Jaspersen SL, Tinker-Kulberg RL, Hwang L, Szidon A, Morgan DO (1998). The Polo-related kinase Cdc5 activates and is destroyed by the mitotic cyclin destruction machinery in S. cerevisiae. Curr Biol 8, 497–507.

Clute P, Pines J (1999). Temporal and spatial control of cyclin B1 destruction in metaphase. Nat Cell Biol 1, 82–87.

Cohen-Fix O, Peters JM, Kirschner MW, Koshland D (1996). Anaphase initiation in Saccharomyces cerevisiae is controlled by the APC-dependent degradation of the anaphase inhibitor Pds1p. Genes Dev 10, 3081–3093.

Cormack BP, Bertram G, Egerton M, Gow NA, Falkow S, Brown AJ (1997). Yeast-enhanced green fluorescent protein (yEGFP): a reporter of gene expression in Candida albicans. Microbiology 143, 303–311.

Eguren M, Manchado E, Malumbres M (2011). Non-mitotic functions of the Anaphase-Promoting Complex. Semin Cell Dev Biol 22, 572–578.

Epp JA, Chant J (1997). An IQGAP-related protein controls actin-ring formation and cytokinesis in yeast. Curr Biol 7, 921–929.

Gadal O, Strauss D, Kessl J, Trumpower B, Tollervey D, Hurt E (2001). Nuclear export of 60s ribosomal subunits depends on Xpo1p and requires a nuclear export sequence-containing factor, Nmd3p, that associates with the large subunit protein Rpl10p. Mol Cell Biol 21, 3405–3415.

Geil C, Schwab M, Seufert W (2008). A nucleolus-localized activator of Cdc14 phosphatase supports rDNA segregation in yeast mitosis. Curr Biol 18, 1001–1005.

Gieffers C, Peters BH, Kramer ER, Dotti CG, Peters JM (1999). Expression of the CDH1-associated form of the anaphase-promoting complex in postmitotic neurons. Proc Natl Acad Sci USA 96, 11317–11322.

Glotzer M, Murray AW, Kirschner MW (1991). Cyclin is degraded by the ubiquitin pathway. Nature 349, 132–138.

Gordon DM, Roof DM (2001). Degradation of the kinesin Kip1p at anaphase onset is mediated by the anaphase-promoting complex and Cdc20p. Proc Natl Acad Sci USA 98, 12515–12520.

Grosskortenhaus R, Sprenger F (2002). Rca1 inhibits APC-Cdh1(Fzr) and is required to prevent cyclin degradation in G2. Dev Cell 2, 29–40.

He J, Chao WC, Zhang Z, Yang J, Cronin N, Barford D (2013). Insights into degron recognition by APC/C coactivators from the structure of an Acm1-Cdh1 complex. Mol Cell 50, 649–660.

Hildebrandt ER, Hoyt MA (2001). Cell cycle-dependent degradation of the Saccharomyces cerevisiae spindle motor Cin8p requires APC(Cdh1) and a bipartite destruction sequence. Mol Biol Cell 12, 3402–3416.

Hood JK, Hwang WW, Silver PA (2001). The Saccharomyces cerevisiae cyclin Clb2p is targeted to multiple subcellular locations by cis- and trans-acting determinants. J Cell Sci 114, 589–597.

Hu D, Liu W, Wu G, Wan Y (2011). Nuclear translocation of Skp2 facilitates its destruction in response to TGFbeta signaling. Cell Cycle 10, 285–292.

Huang JN, Park I, Ellingson E, Littlepage LE, Pellman D (2001). Activity of the APC(Cdh1) form of the anaphase-promoting complex persists until S phase and prevents the premature expression of Cdc20p. J Cell Biol 154, 85–94.

Jaquenoud M, van Drogen F, Peter M (2002). Cell cycle-dependent nuclear export of Cdh1p may contribute to the inactivation of APC/C(Cdh1). EMBO J 21, 6515–6526.

Jaspersen SL, Charles JF, Morgan DO (1999). Inhibitory phosphorylation of the APC regulator Hct1 is controlled by the kinase Cdc28 and the phosphatase Cdc14. Curr Biol 9, 227–236.

Jörgensen PM, Brundell E, Starborg M, Hoog C (1998). A subunit of the anaphase-promoting complex is a centromere-associated protein in mammalian cells. Mol Cell Biol 18, 468–476.

Juang YL, Huang J, Peters JM, McLaughlin ME, Tai CY, Pellman D (1997). APC-mediated proteolysis of Ase1 and the morphogenesis of the mitotic spindle. Science 275, 1311–1314.

Keppler-Ross S, Douglas L, Konopka JB, Dean N (2010). Recognition of yeast by murine macrophages requires mannan but not glucan. Eukaryot Cell 9, 1776–1787.
Ko N, Nishihama R, Tully GH, Ostapenko D, Solomon MJ, Morgan DO, Pringle JR (2007). Identification of yeast IQGAP (Iqg1p) as an anaphase-promoting-complex substrate and its role in actomyosin-ring-independent cytokinesis. Mol Biol Cell 18, 5139–5153.
Kramer ER, Scheuringer N, Podtelejnikov AV, Mann M, Peters JM (2000). Mitotic regulation of the APC activator proteins CDC20 and CDH1. Mol Biol Cell 11, 1555–1569.
Lee KS, Park JE, Asano S, Park CJ (2005). Yeast polo-like kinases: functionally conserved multitask mitotic regulators. Oncogene 24, 217–229.
Melloy PG, Holloway SL (2004). Changes in the localization of the Saccharomyces cerevisiae anaphase-promoting complex upon microtubule depolymerization and spindle checkpoint activation. Genetics 167, 1079–1094.
Michael S, Trave G, Ramu C, Chica C, Gibson TJ (2008). Discovery of candidate KEN-box motifs using cell cycle keyword enrichment combined with native disorder prediction and motif conservation. Bioinformatics 24, 453–457.
Miller JJ, Summers MK, Hansen DV, Nachury MV, Lehman NL, Loktev A, Jackson PK (2006). Emi1 stably binds and inhibits the anaphase-promoting complex/cyclosome as a pseudosubstrate inhibitor. Genes Dev 20, 2410–2420.
Moll T, Tebb G, Surana U, Robitsch H, Nasmyth K (1991). The role of phosphorylation and the CDC28 protein kinase in cell cycle-regulated nuclear import of the S. cerevisiae transcription factor SWI5. Cell 66, 743–758.
Morgan DO (1999). Regulation of the APC and the exit from mitosis. Nat Cell Biol 1, E47–53.
Perzlmaier AF, Richter F, Seufert W (2013). Translation initiation requires cell division cycle 123 (Cdc123) to facilitate biogenesis of the eukaryotic initiation factor 2 (eIF2). J Biol Chem 288, 21537–21546.
Peters JM (2006). The anaphase promoting complex/cyclosome: a machine designed to destroy. Nat Rev Mol Cell Biol 7, 644–656.
Pfleger CM, Kirschner MW (2000). The KEN box: an APC recognition signal distinct from the D box targeted by Cdh1. Genes Dev 14, 655–665.
Pfleger CM, Lee E, Kirschner MW (2001). Substrate recognition by the Cdc20 and Cdh1 components of the anaphase-promoting complex. Genes Dev 15, 2396–2407.
Primorac I, Musacchio A (2013). Panta rhei: the APC/C at steady state. J Cell Biol 201, 177–189.
Prinz S, Hwang ES, Visintin R, Amon A (1998). The regulation of Cdc20 proteolysis reveals a role for APC components Cdc23 and Cdc27 during S phase and early mitosis. Curr Biol 8, 750–760.
Robbins JA, Cross FR (2010). Regulated degradation of the APC coactivator Cdc20. Cell Div 5, 23.
Rudner AD, Murray AW (2000). Phosphorylation by Cdc28 activates the Cdc20-dependent activity of the anaphase-promoting complex. J Cell Biol 149, 1377–1390.
Schwab M, Lutum AS, Seufert W (1997). Yeast Hct1 is a regulator of Clb2 cyclin proteolysis. Cell 90, 683–693.
Schwab M, Neutzner M, Mocker D, Seufert W (2001). Yeast Hct1 recognizes the mitotic cyclin Clb2 and other substrates of the ubiquitin ligase APC. EMBO J 20, 5165–5175.
Shaner NC, Campbell RE, Steinbach PA, Giepmans BN, Palmer AE, Tsien RY (2004). Improved monomeric red, orange and yellow fluorescent proteins derived from Discosoma sp. red fluorescent protein. Nat Biotechnol 22, 1567–1572.
Shannon KB (2012). IQGAP family members in yeast, Dictyostelium, and mammalian cells. Int J Cell Biol 2012, 894817.
Sheff MA, Thorn KS (2004). Optimized cassettes for fluorescent protein tagging in Saccharomyces cerevisiae. Yeast 21, 661–670.
Shirayama M, Toth A, Galova M, Nasmyth K (1999). APC(Cdc20) promotes exit from mitosis by destroying the anaphase inhibitor Pds1 and cyclin Clb5. Nature 402, 203–207.
Shirayama M, Zachariae W, Ciosk R, Nasmyth K (1998). The Polo-like kinase Cdc5p and the WD-repeat protein Cdc20p/fizzy are regulators and substrates of the anaphase promoting complex in Saccharomyces cerevisiae. EMBO J 17, 1336–1349.
Sikorski RS, Hieter P (1989). A system of shuttle vectors and yeast host strains designed for efficient manipulation of DNA in Saccharomyces cerevisiae. Genetics 122, 19–27.
Tian W, Li B, Warrington R, Tomchick DR, Yu H, Luo X (2012). Structural analysis of human Cdc20 supports multisite degron recognition by APC/C. Proc Natl Acad Sci USA 109, 18419–18424.
Topper LM, Campbell MS, Tugendreich S, Daum JR, Burke DJ, Hieter P, Gorbsky GJ (2002). The dephosphorylated form of the anaphase-promoting complex protein Cdc27/Apc3 concentrates on kinetochores and chromosome arms in mitosis. Cell Cycle 1, 282–292.
Visintin R, Craig K, Hwang ES, Prinz S, Tyers M, Amon A (1998). The phosphatase Cdc14 triggers mitotic exit by reversal of Cdk-dependent phosphorylation. Mol Cell 2, 709–718.
Visintin R, Prinz S, Amon A (1997). CDC20 and CDH1: a family of substrate-specific activators of APC-dependent proteolysis. Science 278, 460–463.
Waizenegger IC, Hauf S, Meinke A, Peters JM (2000). Two distinct pathways remove mammalian cohesin from chromosome arms in prophase and from centromeres in anaphase. Cell 103, 399–410.
Wäsch R, Cross FR (2002). APC-dependent proteolysis of the mitotic cyclin Clb2 is essential for mitotic exit. Nature 418, 556–562.
Winey M, Bloom K (2012). Mitotic spindle form and function. Genetics 190, 1197–1224.
Yoshida S, Asakawa K, Toh-e A (2002). Mitotic exit network controls the localization of Cdc14 to the spindle pole body in Saccharomyces cerevisiae. Curr Biol 12, 944–950.
Zachariae W, Schwab M, Nasmyth K, Seufert W (1998). Control of cyclin ubiquitination by CDK-regulated binding of Hct1 to the anaphase promoting complex. Science 282, 1721–1724.
Zachariae W, Shin TH, Galova M, Obermaier B, Nasmyth K (1996). Identification of subunits of the anaphase-promoting complex of Saccharomyces cerevisiae. Science 274, 1201–1204.
Zhou Y, Ching YP, Chun AC, Jin DY (2003). Nuclear localization of the cell cycle regulator CDH1 and its regulation by phosphorylation. J Biol Chem 278, 12530–12536.